Transition from Boundary Lubrication to Hydrodynamic Lubrication of Slider Bearings

Abstract: The transition from boundary lubrication to fully hydrodynamic lubrication is investigated for air-lubricated slider bearings using the electrical resistance method. Intermittent contacts are shown to exist even under conditions for which the numerical solution of the Reynolds equation or white light interferometry predicts steady state spacings in the spacing region from 0.125 to 0.25 μ m. The transition is similar to the one found in the presence of liquid films, being influenced for a given surface roughness of disk and slider by load, speed, and hydrodynamic design.

Introduction

The transition from boundary to hydrodynamic lubrication has been the subject of extensive experimental investigations in the past [1]. The interest in this area is seemingly related to the fact that there are sliding situations in which the desired mode of fully hydrodynamic lubrication is difficult to achieve, and boundary lubrication is present. In this latter case, wear of the sliding surfaces occurs and, therefore, an understanding of the transition from boundary to hydrodynamic lubrication is essential for predicting and minimizing material contacts and wear.

The experimental method most suited for studying the transition from boundary lubrication to hydrodynamic lubrication seems to be the electrical resistance method. Use is made here of the fact that the electrical resistance between conductive sliding surfaces changes from a low value (essentially the contact resistance) to a very high value as boundary lubrication changes into hydrodynamic lubrication. Using this method, Courtney-Pratt and Tudor [2] studied the lubrication between the piston ring and cylinder of a single-cylinder engine. Unexpectedly, an appreciable amount of boundary lubrication was found to exist throughout the entire piston cycle, although a marked decrease in the frequency of material contacts was observed as the velocity of sliding increased. A similar intermittent transition from boundary lubrication to hydrodynamic lubrication was also observed by Tudor [3] in the lubrication of journal bearings, by Crook [4] in the study of gear lubrication, and by Furey [5] in the investigation of contacts between a ball sliding on a lubricated disk. Because these investigations were conducted exclusively in the presence of liquid lubricant films, it may be concluded that the transition from boundary lubrication to hydrodynamic lubrication in the presence of liquid lubricants is indeed intermittent. This conclusion, however, may not be extended a priori to a situation in which the lubricant film is a gas, although similar results may be expected.

This paper describes an investigation of the transition from boundary lubrication to hydrodynamic lubrication for air-lubricated slider bearings, similar to the ones used in magnetic recording disk files. The electrical resistance method is applied to investigate the details of this transition and to examine the relationship between contact frequency, wear, and sliding speed for a given surface roughness of disk and slider. Although the results obtained are seen to depend on the specific hydrodynamic slider design, it is found that the typical transition from continuous sliding to hydrodynamic flying is intermittent and, in this respect, very similar to the transition observed in the presence of fluid films.

Experiment

The experimental setup used throughout the present investigation is shown in Fig. 1. A continuously variable speed motor is used to drive a specially prepared conductive metallic disk that rotates in a test chamber of filtered, slightly pressurized air. Spring-loaded against the disk is a 52100 steel slider, made up of three individual taper-flat air-bearing surfaces, specifically fabricated

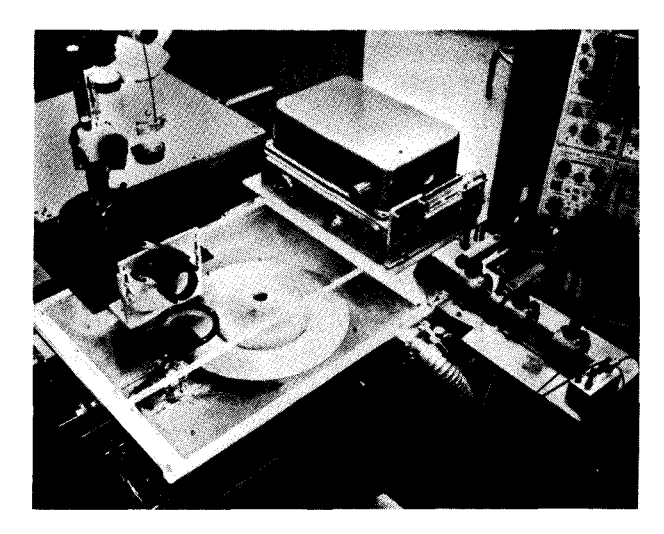


Figure 1 Experimental apparatus used in the lubrication study.

for this investigation and shown in Fig. 2. The slider load, applied by lowering the slider support against the disk, is measured by means of strain gauges mounted on the suspension spring.

The rotating disk is maintained at solid ground potential through a connection in a mercury bath mounted on the axis of the spindle shaft. Adequate grounding was found to be essential for eliminating electrical noise due to charge buildup from the driving belt. Contacts between the slider and the disk are detected and counted using the circuit shown in Fig. 3. A low voltage is applied across the slider-disk gap, which is in parallel with a load resistor $R_{\rm L}$. Thus, a near short circuit results with low gap resistance if the slider and the disk are in direct contact, and an open-circuit branch exists if the slider and the disk are separated. It is apparent that this change in gap resistance can be detected as a voltage change across the load resistor R_L . That is, a voltage drop across $R_{\rm L}$ equal to the applied potential corresponds to separation between the slider and the disk, whereas near zero voltage corresponds to slider/disk contacts. Although this arrangement worked satisfactorily, amplification of the voltage across R_L was found practical for displaying the signal on the oscilloscope or counting contact pulses on the counter.

The presence of two voltage stages is somewhat modified in practice by the appearance of intermediate voltage levels due to the nonzero contact resistance between slider and disk. It is therefore not possible to determine whether voltage pulses below a certain level correspond to contacts with high contact resistance or to noise in the circuit, and an arbitrary threshold value corresponding to 10 percent of the maximum voltage was chosen as the cutoff value for pulse counting. A synchronized signal derived from a Fotonic probe was used to trigger the

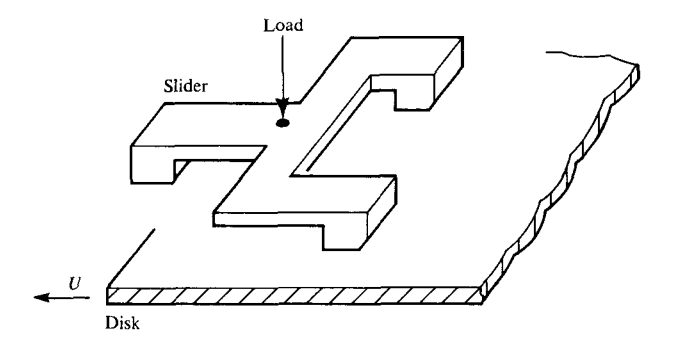


Figure 2 Taper-flat steel slider used in the experimental study.

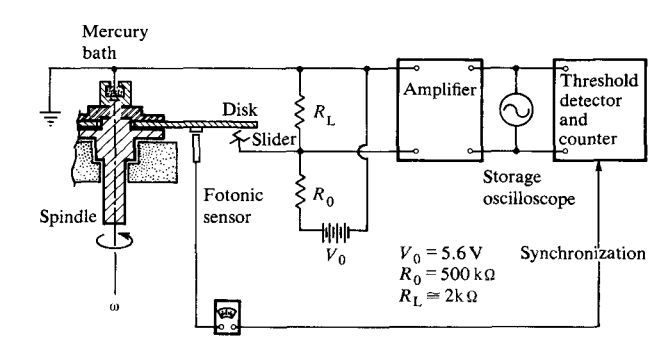


Figure 3 Circuit for detecting and counting the contacts between slider and disk.

counter circuit to enable counting of contact pulses per disk revolution. This synchronized signal was also used for the measurement of the disk rotational speed.

For the circuit parameters in Fig. 3 we calculate that a slider-disk potential of 20 mV is small enough to prevent voltage discharge through air gaps larger than approximately 6 nm, assuming a breakdown electrical field strength for air of 3×10^4 V/cm [6]. Indeed, we determined in an auxiliary experiment, where we used the high-precision mechanical movement of a laser translation stage to traverse a disk segment against the slider surface, that no discharge occurred for a potential of 20 mV for stationary separations equal to or larger than approximately 25 nm. Hence, the voltage pulses recorded by the scope or the threshold detector are truly the result of surface contacts between slider and disk.

Prior to the experiment, the three pads of the slider were lapped flat to within a 50 nm peak-to-valley surface roughness across the flat portion, leaving small tapered sections at the leading edges. The steady-state flying characteristic of the slider was then determined on a glass disk using white light interferometry. The glass disk used for the spacing calibration was a precision finished disk with less than 25 nm peak-to-valley surface roughness. Since the slider-disk separation was

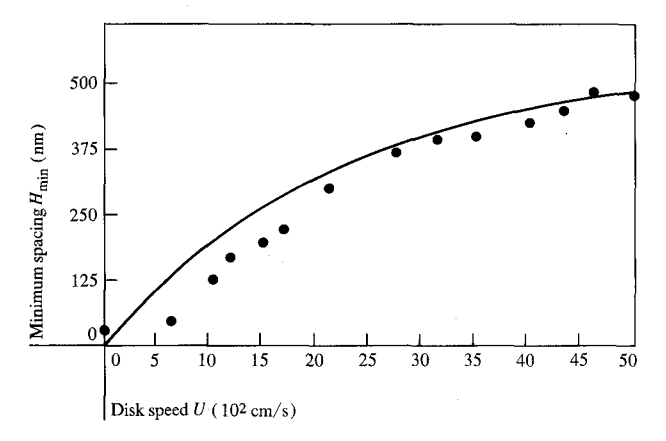


Figure 4 Comparison between computed and measured spacings for rear pad of typical taper-flat slider. The heavy line is the result of numerical calculation; the dots represent the results of white light measurements on a glass disk.

in general less than one μ m, colored interference fringes were present, thus allowing the determination of flying heights with an accuracy of ± 25 nm.

A comparison between measured and numerically calculated spacings for the rear pad of a typical taper-flat slider is shown in Fig. 4. We observe that at low velocities the measured spacings depart from the numerically predicted ones, seemingly because of material interactions due to surface roughness and increased inaccuracy of the theoretical model which assumes perfectly flat surfaces. After the steady state flying characteristics was established, the glass disk was replaced by a metallic disk, thus permitting detection of slider/disk contacts and the investigation of the nature of the transition from continuous sliding to steady flying.

Experimental results

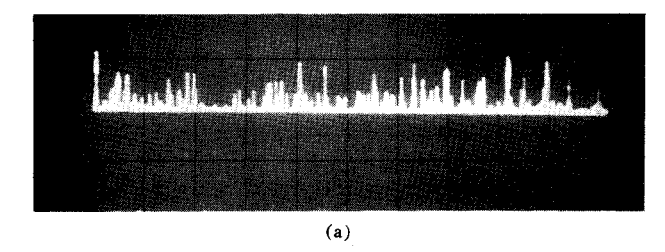
A typical set of voltage output traces is shown in Fig. 5 as a function of velocity, using the slider depicted in Fig. 2. It can be seen clearly from these photographs that contacts, corresponding to narrow spikes, are present over most of the examined speed range. These contacts decrease in number as well as in magnitude as the velocity increases, and disappear completely above approximately 2000 cm/s. A similar behavior is also observed if the load of the slider is increased, although in this case the absence of contacts is observed at a much higher disk velocity. Characteristic of all the observed traces is the random nature of the pulses and the weak dependence of the pulse width on the sliding speed.

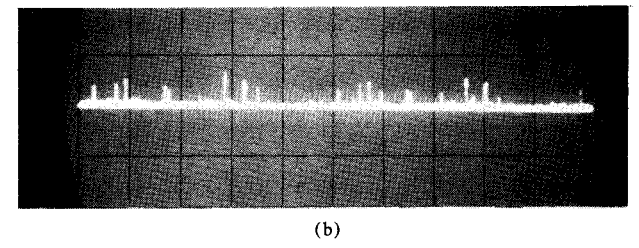
When the number of contact pulses per revolution is plotted from photographs similar to the ones in Fig. 5, the lower curve in Fig. 6 is obtained. A similarly shaped curve is also obtained when the numerical readings from the threshold counter are plotted, as can be seen from the upper curve in the same figure. Since in either count-

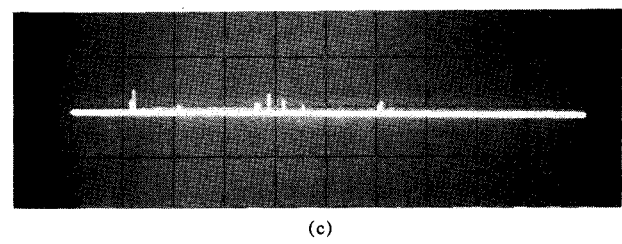
ing method a somewhat arbitrary cutoff value is used for voltage spikes to be counted as contacts, it is apparent that physical significance should be attached primarily to the general dependence of contacts on speed rather than to the absolute magnitude of counts. Clearly, the absence of contacts above approximately 2000 cm/s indicates the presence of a fully established hydrodynamic air film capable of supporting the total applied load, while the region to the left of 2000 cm/s corresponds to the transition region. Thus, contacts between the slider and the disk are observed even at velocities where the numerical solution of the Reynolds equations predicts a steady state separation of approximately 0.125 to 0.250 μ m (Fig. 4).

Because white light interferometry data for the dependence of flying height on velocity agree well with the numerical predictions for velocities above 1250 cm/s, a seemingly large discrepancy is observed between the predictions from the resistance method and either white light interferometry or numerical solution. This, however, should be looked upon not as discrepancy, but rather as complementary information. That is, contacts occurring in the transition region simply cannot be detected with interferometric methods because of the limited frequency resolution of the human eye, although in an average sense there is a steady state separation between the slider and the disk. Furthermore, the peak-to-valley surface roughness value of the glass disk (25 nm) is appreciably less than that of the metal disk (175 nm) and thus differences in the flying behavior may partially be related to the different surface roughness. However, even if we used a glass disk having a surface roughness identical to that of the metal disk, contacts between the slider and the disk could not be detected visually. This is so because contacts between surfaces occur generally only at a limited number of microscopically small asperities, and at the magnification used in the interferometric work these contact areas would be too small to be noticeable. From this viewpoint, then, the results of the electrical resistance method should be taken as additional detailed information that is not obtainable by other methods.

It is apparent that continued contact between the slider and the disk results in wear of the contacting surfaces. Therefore, additional information concerning the transition to fully hydrodynamic lubrication may be obtained by measuring the amount of wear of the slider and the disk. In Fig. 7 the volume V, worn off the trailing pad of the slider shown in Fig. 2, is plotted as a function of velocity for a constant sliding distance s. A particulate disk with a polymeric overcoat, containing finely dispersed alumina particles as the primary abrasive material, was used in this study because it was found that wear, seemingly abrasive in nature, occurs for the parti-







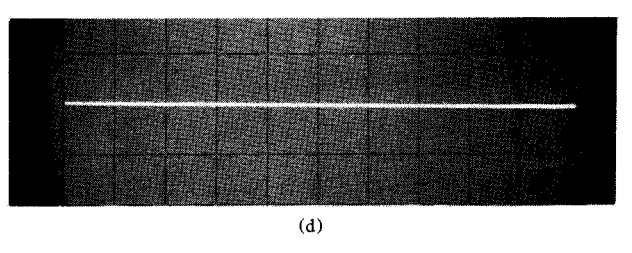


Figure 5 Storage oscilloscope voltage output traces for contact pulses, for the slider depicted in Figure 2. Ordinate, 0.5 V/div; abscissa, 20 ms/div.

ω in rpm		Disk speed U in cm/s
a)	100	160
b)	600	960
c)	1200	1920
d)	1500	2400

culate coating/steel slider interface mainly in the form of slider wear. In particular, slider wear was seen to consist of a gradual, uniform removal of material from the flat portion of the bearing surfaces [7], thus making it possible to calculate the total amount of wear by measuring the increase in flat lengths, i.e.,

$$V = (B^2 - B_0^2)l \cdot H_0/2(b - B_0), \tag{1}$$

where

 B, B_0 are the new and original length of the flat, b, l are the total length and width of the slider pad, and H_0 is the original taper height.

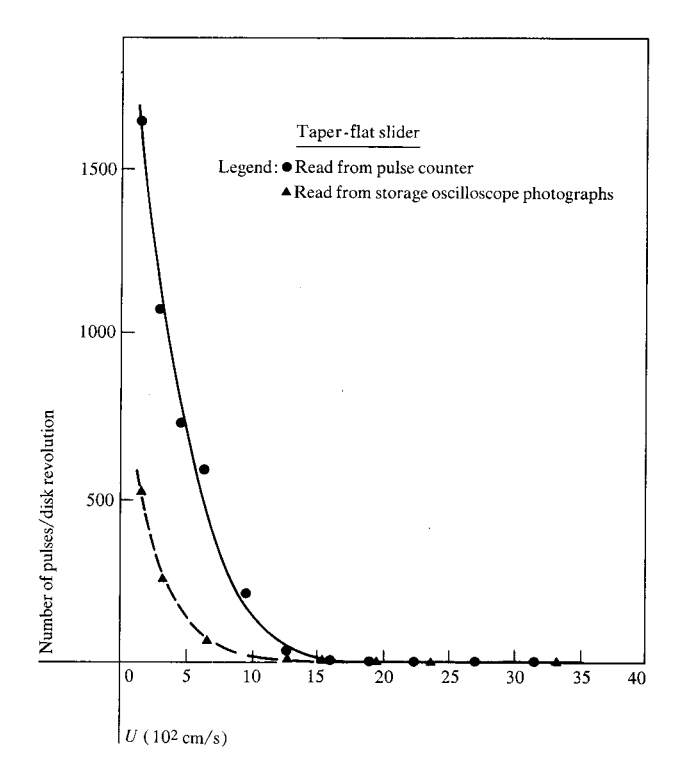


Figure 6 Contact pulses for taper-flat slider, based on data in Figure 5.

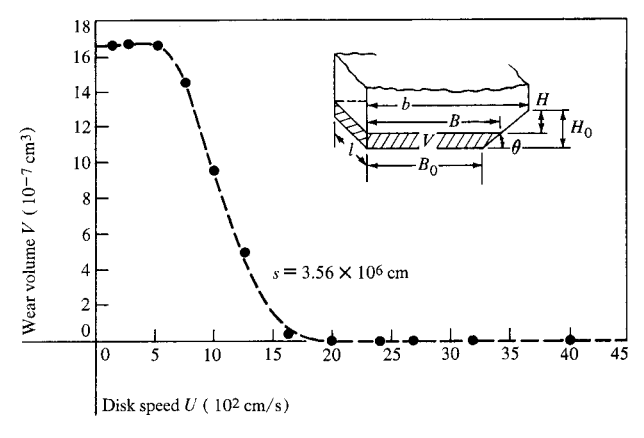


Figure 7 Wear of the trailing pad of the slider in Figure 2, at a constant distance of travel.

From Fig. 7 it is observed that a marked decrease in the amount of wear per sliding distance occurs for velocities above 500 cm/s, and that no measureable wear is noticed for velocities above 2000 cm/s. This result is in excellent agreement with the results from the electrical resistance method, which predicts no material interactions, e.g., wear, above sliding speeds of 2000 cm/s. The excellent quantitative agreement between the results of the electrical resistance method and the wear results seems surprising at first, because two different types of disks, metallic and particulate, were used.

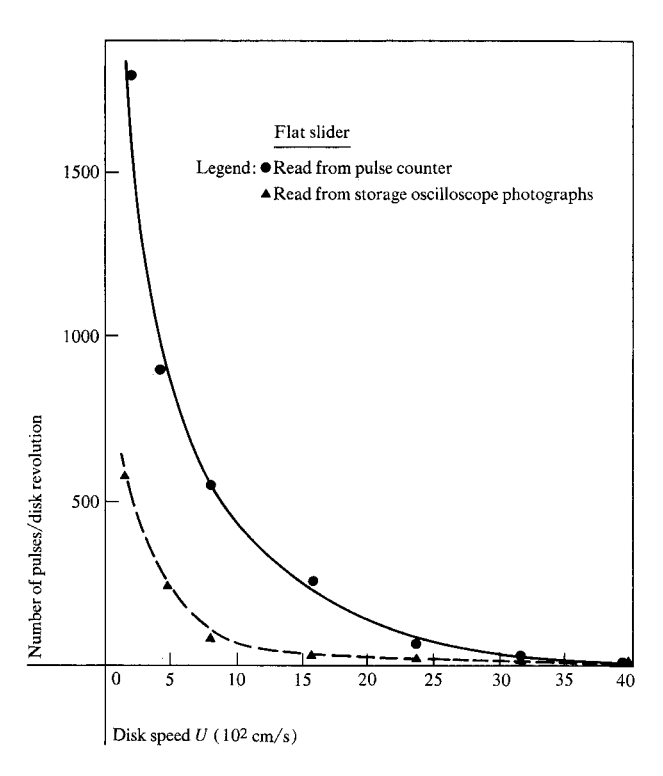


Figure 8 Contact pulses for a nearly flat tripad slider.

However, because the surface roughness of both disks was approximately the same, it is most likely that there should not be major differences in the flying characteristic of the slider.

From the results presented above, it is apparent that the transition between continuous sliding and steady flying is intermittent and is largely influenced by velocity for constant load. There is, however, an equally important dependence of the transition characteristic on the hydrodynamic slider design. This is shown clearly by comparing Fig. 8 (which represents a plot of contact frequency vs sliding speed for a nearly flat tripad slider) with Fig. 6. Figure 8 shows that contacts occur throughout the investigated velocity range, although their number decreases toward zero at speeds higher than those experienced with the taper flat sliders. Thus, the dependence of contact frequency on velocity is similar to previous findings, although the transition region extends to much higher velocities.

Since interferometric data for the almost-flat slider show that even at very high velocities the air bearing between slider and disk is of the order of only $0.125~\mu m$, the occurrence of contacts is not too surprising. In fact, based on the latter result and additional experiments where we changed the load at constant velocity, we may conclude that the transition between sliding and flying is closely related for constant surface roughness and constant slider dynamics to the average air bearing spacing

between slider and disk. This finding implies, of course, that the transition from boundary lubrication to hydrodynamic lubrication is a function of load, velocity and hydrodynamic slider design.

Theoretical considerations and discussion

The analytical description of the slider bearing behavior in the transition region is complicated because of the coupling of two very different physical phenomena. That is, the parameters governing intermittent contacts are associated with material properties, slider dynamics, surface roughness, and wear, whereas the parameters describing flying are associated mainly with the fluid properties of the air film between slider and disk, slider geometry, and slider dynamics. The flying characteristic, however, is intimately related to the type and strength of contacts. Likewise, the contact strength and frequency depends on the stiffness and hence properties of the air film. Only in the limiting cases of very small and very large velocities do the equations governing the transition phenomena become uncoupled because of (a) the negligible effect of hydrodynamic forces at low speeds, and (b) the absence of contacts in the high speed limit. These limiting cases are more amenable to analytical solutions, and we discuss them first before analyzing the more complicated problem of the transition region.

Considering the low-speed limiting case first, we note that in the absence of hydrodynamic forces the total slider load N is supported by individual asperities, thus leading to wear under sliding conditions. It was suggested previously that wear in our particular experiment is abrasive in nature. This, then, implies that the wear behavior of the slider in the low speed case should be described by the equations governing abrasive wear [8], i.e.,

$$V = k(N/p_{\rm m})s \tag{2}$$

or, for a fixed load N and constant hardness $p_{\rm m}$,

$$V = k's, (3)$$

where k and k' are constants of proportionality and s is the sliding distance. That is, as long as hydrodynamic effects are negligible, the volume V worn off the slider should be invariant for a constant length of sliding. It is apparent from Fig. 7 that wear of the slider at a fixed sliding distance is indeed constant and independent of the velocity up to approximately 500 cm/s; thus, excellent agreement between theoretical predictions and experiment exists in the low-speed limiting case.

The limiting case of high velocities, corresponding to steady separation between the slider and the disk, can be obtained by solving the Reynolds equation [9] that relates the pressure p under the bearing surface to the spacing h, velocity U, and viscosity η . If the minimum spacing h decreases to very small values at which the

ratio of the molecular mean free path λ and the spacing h becomes larger than $O(10^{-2})$ over an appreciable region of the slider bearing, corrections due to slip flow at the boundaries must be taken into account [10]. In this case the modified Reynolds equation takes the form

$$\frac{\partial}{\partial x} \left[ph^3 \frac{\partial p}{\partial x} \left(1 + 6 \frac{\lambda}{h} \right) \right] + \frac{\partial}{\partial y} \left[ph^3 \frac{\partial p}{\partial y} \left(1 + 6 \frac{\lambda}{h} \right) \right]$$

$$= 12\eta \frac{\partial}{\partial t} (ph) + 6\eta U \frac{\partial}{\partial x} (ph), \tag{4}$$

where x and y denote bearing coordinates and t denotes time. As we have seen previously, very good agreement in the high speed limit exists with experimental measurements, and it appears that the steady state Reynolds equation sufficiently describes the physical situation in this limiting case.

Although the solution of the steady state equation is appropriate for large velocities and very smooth surfaces, in the case of appreciable slider dynamics the time-dependent Reynolds equation and the dynamic equations of motion [11] of the slider must be used to describe the physical situation. The dynamic equations of the slider shown in Fig. 9 assume then the following form:

$$\begin{split} m\ddot{z} &= \sum_{i=1}^{3} W_{i}(t) - N(t), \\ I_{y}\ddot{a} &= N(t)x_{N} - \sum_{i=1}^{3} W_{i}(t)x_{i} - \sum_{i=1}^{3} F_{i}(t)z_{i} - K_{\alpha}(\alpha - \alpha_{0}), \\ I_{x}\ddot{\beta} &= N(t)y_{N} + \sum_{i=1}^{3} W_{i}(t)y_{i} - K_{\beta}(\beta - \beta_{0}). \end{split} \tag{5}$$

It seems justifiable to postulate that Eqs. (4) and (5) are valid not only for the description of the dynamic behavior of the slider bearing, but also for the description of the slider motion between intermittent contacts. The equations, however, are not valid for the intermittent contact itself. To describe contacts we may proceed in the following way. We first calculate the dynamic flying height from Eqs. (4) and (5) by simultaneous numerical solution. Whenever the calculated spacing is less than the sum of the surface roughness of the disk and the slider, an intermittent contact is assumed by including the effect of a normal impact force $N^*(t)$ in Eq. (5). Thereafter the simultaneous numerical solution of Eqs. (4) and (5) is continued until the next potential contact situation is encountered.

It will be shown in the following that the normal impact force $N^*(t)$ is equivalent to a step change in vertical velocity at the time of the impact, and therefore the impact can be represented by new initial conditions for Eq. (4). From our experimental data we observe that the duration of contacts is typically of $O(10^{-4})$ s. In addition, the time variation of electrical conductivity, which

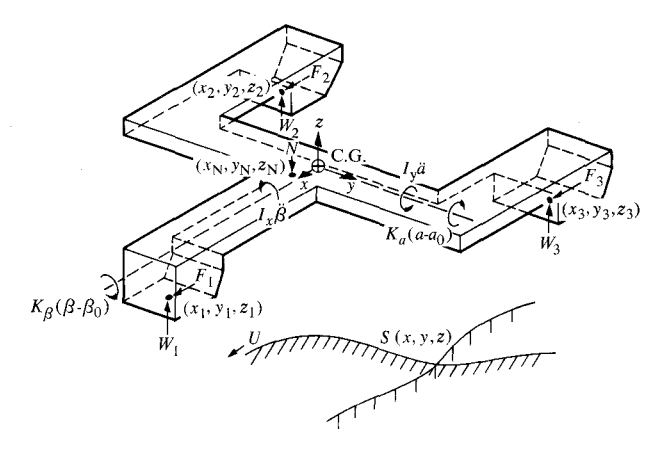


Figure 9 Schematic for slider dynamics. I_xI_y is the moment of inertia; K_α , K_β , spring stiffness; α , β , pitch and roll angles, respectively; N, F, W, forces on slider.

may be assumed to be proportional to the time variation of the contact force $N^*(t)$ [12], is determined experimentally. In particular, it is found that the variation of $N^*(t)$ can be approximated sufficiently accurately, in general, by the functional relationship

$$N^*(t) = \begin{cases} \left(\frac{t}{t_{\rm M}}\right)' \cdot N_{\rm max}^* & \text{for } t < t_{\rm M}, \\ \left(\frac{t_{\rm T} - t}{t_{\rm T} - t_{\rm M}}\right) \cdot N_{\rm max}^* & \text{for } t_{\rm M} < t < t_{\rm T}, \end{cases}$$

$$(6)$$

where $t_{\rm T}$ denotes the total impact time and $t_{\rm M}$ denotes the time from the beginning of the impact up to the point when the velocity v of the impacting slider has come to zero. Thus it is apparent that the first part of the impulse curve, for which $0 < t < t_{\rm M}$, describes the force during the elastic and possibly plastic deformation during the impact, while the latter part of the impulse curve, for which $t_{\rm M} < t < t_{\rm T}$, represents the elastic rebound, which is responsible for the final impulse given to the slider. For the first part of the impact we obtain from Eq. (6) and Newton's second law that

$$mv_0 = -N_{\text{max}}^* t_{\text{M}}/2,$$
 (7)

where v_0 is the initial relative velocity between the slider and the disk in the z direction at impact. Likewise, we obtain for the rebound part of the impact that

$$mv_{\rm T} = N_{\rm max}^* \left(\frac{t_{\rm T} - t_{\rm M}}{2}\right),\tag{8}$$

where $v_{\rm T}$ denotes the separation velocity of the slider at the end of the impact.

Combining Eqs. (7) and (8), we obtain

$$v_{\mathrm{T}} = -v_{\mathrm{o}} \cdot \left(\frac{t_{\mathrm{T}} - t_{\mathrm{M}}}{t_{\mathrm{M}}}\right). \tag{9}$$

539

Thus, the final separation velocity at the end of the impluse can be calculated by merely using the experimentally determined times $t_{\rm T}$ and $t_{\rm M}$, i.e., contact between the slider and the disk can be approximated as a step change in the z component of the relative velocity between the slider and the disk. It should be pointed out that in the above model no specific assumptions concerning the nature of the impact are made, and thus the model is valid for elastic as well as plastic impacts. Currently, numerical simulation of the slider behavior in the transition zone is being carried out and will be reported in a later publication.

Summary

The transition from boundary to hydrodynamic lubrication for air-lubricated slider bearings was investigated using the electrical resistance method. Intermittent contacts were found to occur even under conditions for which white light interferometry as well as numerical analysis predicts steady state separations of 0.125 to 0.250 μ m. It appears that this discrepancy is caused (a) by the neglect of surface roughness in the steady state numerical analysis, and (b) by the use of a very smooth glass disk for the flying height measurement, and by the limited resolution of the human eye in detecting small asperity contacts or high frequency separation changes using white light interferometry.

The experimental results are seen to be in excellent agreement with the theoretical solution for the limiting cases of small and large velocities corresponding to (a) a wear situation under steady sliding without hydrodynamic forces, and (b) fully hydrodynamic flying and absence of contacts. While these limiting cases can be de-

scribed by steady state equations, in the transition region the time-dependent Reynolds equation must be considered together with the impact equations and the dynamic equations of motion.

Acknowledgments

We thank R. C. Durbeck for helpful discussions and A. Juliana for his help in building the electronic circuits.

References

- 1. A. Cameron, *The Principles of Lubrication*, Ch. 10., John Wiley and Sons, Inc., New York, 1966.
- J. S. Courtney-Pratt and G. K. Tudor, Proc. Inst. Mech. Eng. 155, 293 (1946).
- 3. G. K. Tudor, C.S.I.R. (Australia) Tribophysics Division Report A, 155 (1947).
- 4. A. W. Crook, Proc. Inst. Mech. Eng. 171, 187 (1957).
- 5. M. J. Furey, Trans. A.S.L.E. 4, 1 (1961).
- J. D. Cobine, Gaseous Conductors, Ch. 7, Dover Publications, Inc., New York, 1958.
- 7. F. E. Talke and R. C. Tseng, Wear 28, 15 (1974).
- 8. E. Rabinowicz, Friction and Wear of Materials, John Wiley and Sons, Inc., New York, 1966.
- 9. W. A. Gross, *Gas Film Lubrication*, Ch. 2, John Wiley and Sons, Inc., New York, 1962.
- 10. A. Burgdorfer, J. Basic Eng., Trans. ASME, 81, 94 (1959).
- 11. T. Tang, Journal of Lubrication F93, No. 2, 272 (1971).
- E. P. Bowden, and D. Tabor, The Friction and Lubrication of Solids, Vol. 1, Clarendon Press, Oxford, 1964, Ch. 12.

Received March 18, 1974

The authors are located at the IBM Research Division Laboratory, Monterey and Cottle Roads, San Jose California, 95193